ANL/ET/CP-100308

A Fracture Mechanics Approach for Estimating Fatigue Crack Initiation in Carbon and Low-Alloy Steels in LWR Coolant Environments*

H. B. Park[1] and O. K. Chopra[2]

[1]Korea Power Engineering Company, Inc.,
360-9 Mabukri, Kusongmyon, Yonginshi, Kyunggido, Korea

[2]Energy Technology Division, Argonne National Laboratory
9700 South Cass Avenue, Argonne, Illinois 60439 USA

January 2000

To be presented at 2000 ASME Pressure Vessels and Piping Conference, July 23-27, 2000, Seattle.

*Work supported by the International Atomic Energy Agency Fellowship Program, administered by The National Academy of Sciences – National Research Council (NAS-NRC), under a contract with the U.S. Government.

DISCLAIMER

DISCLAIMER

A FRACTURE MECHANICS APPROACH FOR ESTIMATING FATIGUE CRACK INITIATION IN CARBON AND LOW–ALLOY STEELS IN LWR COOLANT ENVIRONMENTS

Heung–Bae Park[1] and Omesh K. Chopra[2]
[1]Korea Power Engineering Company, Inc.,
360–9 Mabukri, Kusongmyon, Yonginshi, Kyunggido, Korea

[2]Energy Technology Division, Argonne National Laboratory
9700 South Cass Avenue, Argonne, Illinois 60439 USA

ABSTRACT

A fracture mechanics approach for elastic-plastic materials has been used to evaluate the effects of light water reactor (LWR) coolant environments on the fatigue lives of carbon and low-alloy steels. The fatigue life of such steel, defined as the number of cycles required to form an engineering–size crack, i.e., 3–mm deep, is considered to be composed of the growth of (a) microstructurally small cracks and (b) mechanically small cracks. The growth of the latter was characterized in terms of ΔJ and crack growth rate (da/dN) data in air and LWR environments; in water, the growth rates from long crack tests had to be decreased to match the rates from fatigue S–N data. The growth of microstructurally small cracks was expressed by a modified Hobson relationship in air and by a slip dissolution/oxidation model in water. The crack length for transition from a microstructurally small crack to a mechanically small crack was based on studies on small crack growth. The estimated fatigue S-N curves show good agreement with the experimental data for these steels in air and water environments. At low strain amplitudes, the predicted lives in water can be significantly lower than the experimental values.

INTRODUCTION

The formation of surface cracks and their growth as shear (stage I) and tensile (stage II) cracks to an engineering size constitute the fatigue life of a material, which is represented by the stress or strain amplitude vs. fatigue life (S–N) curves. These curves define, for a given stress or strain amplitude, the number of cycles needed to form an engineering–size, i.e., ≈3–mm, crack.

Cyclic loadings on a structural component occur because of changes in the mechanical and thermal loadings as the system goes from one load set (e.g., pressure, temperature, moment, and force loading) to any other load set. For each load set, an individual fatigue usage factor is determined by the ratio of the number of cycles anticipated during the lifetime of the component to the allowable cycles. Figures I–9.1 through I–9.6 of Appendix I to Section III of the ASME Boiler and Pressure Vessel Code specify fatigue design curves that define the allowable number of cycles as a function of applied stress amplitude. The cumulative usage factor (CUF) is the sum of the individual usage factors, and the ASME Code Section III requires that the CUF at each location must not exceed 1.

The current ASME Code design fatigue curves are based on strain–controlled fatigue tests of small polished specimens in air at room temperature. The design fatigue curves have been obtained by first adjusting the best-fit curves to the experimental data for mean stress effects and then decreasing the adjusted curves by a factor of 2 on stress or 20 on cycles, whichever was more conservative, at each point on the curve. These factors were intended to account for the differences and uncertainties in relating fatigue lives of laboratory test specimens to those of actual reactor components. The factors of 2 and 20 are not safety margins but rather conversion factors that must be applied to the experimental data to obtain reasonable estimates of the lives of actual reactor components.

The effects of light water reactor (LWR) coolant environment on fatigue resistance of a material are not explicitly addressed in the Code design fatigue curves. Existing fatigue S–N data illustrate potentially significant effects of LWR coolant environments on the fatigue resistance of carbon and low–alloy steels [1–5]. The key parameters that influence fatigue life in LWR environments are temperature, dissolved oxygen (DO) level in water, loading or strain rate, sulfur content in steel, and strain (or stress) amplitude. Under certain environmental and loading conditions, the environmental effects alone substantially exceed the factor of 20 on life that is used to account for the differences between specimen tests and component behavior.

During fatigue loading of smooth test specimen, surface cracks 10 μm or longer form quite early in life (i.e., <10% of life) at surface irregularities/discontinuities either already in existence or produced by

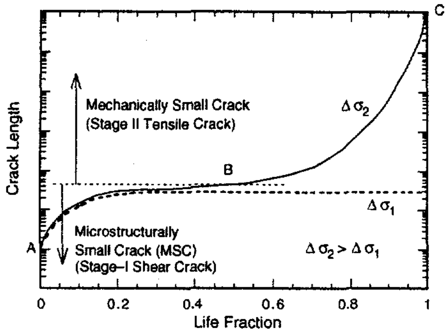

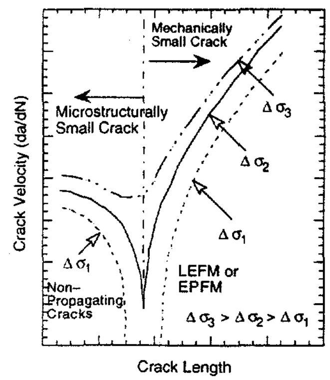

Figure 1. Schematic illustration of growth of short cracks in smooth specimens

slip bands, grain boundaries, second phase particles, etc. [6–9]. Growth of these surface cracks may be divided into two regimes; (a) initial period involving growth of microstructurally small cracks (MSCs) that is very sensitive to microstructure and is characterized by decelerating crack growth (region AB in Fig. 1), and (b) propagation period involving growth of mechanically small cracks that can be predicted by fracture mechanics methodology and is characterized by accelerating crack growth (region BC in Fig. 1). Mechanically small cracks correspond to Stage II, or tensile, cracks characterized by striated crack growth and a fracture surface normal to the maximum principal stress. Conventionally, the former has been defined as the "initiation" stage and is considered to be sensitive to the stress or strain amplitude, and the latter has been defined as the "propagation" stage and is less sensitive to the strain amplitude. The characterization and understanding of both the crack initiation and crack propagation stage are important for accurate estimates of the fatigue lives of structural materials.

Reduction in life in LWR environments may arise from an increase in growth rates of cracks during the initial stage of microstructurally small crack and shear crack growth and/or during the final stage of mechanically small crack and tensile crack growth. Studies on crack initiation in smooth fatigue specimens indicate that the decreased lives of carbon and low–alloy steels in LWR environments are caused primarily by the effects of environment on the growth of cracks < 100 µm deep [2,5,8]. Also, metallographic examination of the test specimens indicate that in high–DO water, growth of MSCs occurs by slip oxidation/dissolution.

The objective of this paper is to use crack growth data and fracture mechanics analyses to examine the fatigue S-N behavior of carbon and low-alloy steels in air and LWR environments. Fatigue life is considered to be composed of the growth of (a) microstructurally small cracks and (b) mechanically small cracks. The growth of the latter has been characterized in terms of the J–integral range ΔJ and crack growth rate (CGR) data in air and LWR environments. The growth of microstructurally small cracks is expressed by a modified Hobson relationship [10,11] in air and by the slip dissolution/oxidation process [12] in water.

FATIGUE S–N DATA IN LWR ENVIRONMENTS

The fatigue lives of both carbon and low–alloy steels are decreased in LWR environments; the reduction in life depends on temperature, strain rate, dissolved oxygen (DO) level in water, and sulfur content of the steel [1–5,13,14]. Fatigue life is decreased significantly when four conditions are satisfied simultaneously, viz., strain amplitude, temperature, and DO in water are above a minimum level, and strain rate is below a threshold value. Although the microsturctures and cyclic–hardening behavior of carbon and low–alloy steels differ significantly, environmental degradation of fatigue life of these steels is very similar. For both steels, only moderate decrease in life (by a factor of <2) is observed when any one of the threshold conditions is not satisfied, e.g., temperature <150°C, strain rate >1%/s, DO levels <0.05 ppm, or applied strain range is below a critical value. The effects of the critical parameters on fatigue life and their threshold values are summarized below.

(a) *Strain:* A minimum threshold strain is required for environmental effects to occur; limited data suggest that the threshold value is ≈20% higher than the fatigue limit for the steel.
(b) *Strain Rate*: Environmental effects occur primarily during the tensile–loading cycle, and at strain levels greater than the threshold value required to rupture the surface oxide film. When all other threshold conditions are satisfied, fatigue life decreases logarithmically with decreasing strain rate below 1%/s; the effect saturates at ≈0.001%/s.
(c) *Temperature*: When other threshold conditions are satisfied, fatigue life decreases linearly with temperature above 150°C.
(d) *Dissolved Oxygen in Water*: When other threshold conditions are satisfied, fatigue life decreases logarithmically with DO above 0.05 ppm; the effect saturates at ≈0.5 ppm DO.
(e) *Sulfur Content of Steel*: The effect of S content on fatigue life depends on the DO content in water. When all threshold conditions are satisfied and DO level is between 0.05–0.2 ppm, fatigue life decreases with increasing S content. Environmental effects saturate at an S content of ≈0.015 wt.%. At high DO contents, e.g., >0.5 ppm, fatigue life seems to be insensitive to S content in the range of 0.002–0.015 wt.% [15].

Statistical models based on the existing fatigue S–N data have been developed for estimating fatigue lives of carbon and low–alloy steels in air and LWR environments [2,3,5]. In air, the fatigue data for carbon steels are best represented by

$$\ln(N) = 6.564 - 1.975 \ln(\varepsilon_a - 0.113) - 0.00124\,T \qquad (1a)$$

and for low–alloy steels by

$$\ln(N) = 6.627 - 1.808 \ln(\varepsilon_a - 0.151) - 0.00124\,T, \qquad (1b)$$

where N is fatigue life of a smooth test specimen, T is temperature (°C), and ε_a is applied strain amplitude (%). In LWR environments, the fatigue data for carbon steels are best represented by

$$\ln(N) = 6.010 - 1.975 \ln(\varepsilon_a - 0.113) + 0.101\, S^* T^* O^* \dot{\varepsilon}^* \quad (2a)$$

and for LASs by

$$\ln(N) = 5.729 - 1.808 \ln(\varepsilon_a - 0.151) + 0.101\, S^* T^* O^* \dot{\varepsilon}^*, \quad (2b)$$

where S^*, T^*, O^*, and $\dot{\varepsilon}^*$ are transformed sulfur content, temperature, DO, and strain rate, respectively, defined as follows:

$$\begin{array}{lll} S^* = 0.015 & (\text{DO} > 1 \text{ ppm}) & \\ S^* = S & (\text{DO} \le 1 \text{ ppm and } 0 < S \le 0.015 \text{ wt.\%}) & \\ S^* = 0.015 & (\text{DO} \le 1 \text{ ppm and } S > 0.015 \text{ wt.\%}) & (3a) \end{array}$$

$$\begin{array}{lll} T^* = 0 & (T < 150°C) & \\ T^* = T - 150 & (T = 150\text{–}350°C) & (3b) \end{array}$$

$$\begin{array}{lll} O^* = 0 & (\text{DO} < 0.05 \text{ ppm}) & \\ O^* = \ln(\text{DO}/0.04) & (0.05 \text{ ppm} \le \text{DO} \le 0.5 \text{ ppm}) & \\ O^* = \ln(12.5) & (\text{DO} > 0.5 \text{ ppm}) & (3c) \end{array}$$

$$\begin{array}{lll} \dot{\varepsilon}^* = 0 & (\dot{\varepsilon} > 1\%/s) & \\ \dot{\varepsilon}^* = \ln(\dot{\varepsilon}) & (0.001 \le \dot{\varepsilon} \le 1\%/s) & \\ \dot{\varepsilon}^* = \ln(0.001) & (\dot{\varepsilon} < 0.001\%/s). & (3d) \end{array}$$

The discontinuity in the value of O^* at 0.05 ppm DO is due to an approximation and does not represent a physical phenomenon.

INITIAL CRACK SIZE

Studies on crack initiation in smooth fatigue specimens indicate that surface cracks form quite early in life. Smith et al. [16] detected 10–µm deep surface cracks at temperature up to 700°C in Waspalloy. Hussain et al. [17] examined the growth of ≈20–µm–deep surface cracks through four or more grains. Tokaji et al. [6,7,18,19] defined crack initiation as the formation of a 10–µm–deep crack. Gavenda et al. [8] reported that in room–temperature air, 10–µm–deep cracks form early during fatigue life, i.e., <10% of fatigue life. Suh et al. [9,20] reported that a crack is said to have initiated when any crack-like mark grows across a grain boundary, or when the separation of grain boundaries becomes clear. Based on these results, it is reasonable to assume the initial depth of MSCs to be ≈10 µm.

TRANSITION FROM MICROSTRUCTURALLY SMALL TO MECHANICALLY SMALL CRACK

Various criteria may be used to define the crack length for transition from MSC to mechanically small crack. They may be related to the (a) plastic zone size, (b) crack length versus fatigue life (a–N) curve, (c) Weibull distribution of the cumulative probability of fracture, (d) stress range versus crack length curve, or (e) grain size. The results indicate that the crack length for transition from microstructurally small to mechanically small crack depends on applied stress and microstructure of the material.

(a) de los Rios et al., [21,22] and Lankford [23–25] defined the transition from small to large cracks as the crack length at which the size of the linear elastic fracture mechanics (LEFM) plastic zone exceeds a grain diameter.

(b) Obrtlik et al. [26] divided the fatigue crack length, a, versus fatigue life, N, curves into two regimes: (a) microstructurally small cracks, in which the dependence of crack length on fatigue life can be represented by a straight line; and (b) mechanically small cracks, in which fatigue crack growth is represented by an exponential function fit of the experimental data.

(c) Suh et al. [9,20] used the knee in the Weibull distribution of cumulative probability of fracture to define the transition from shear crack growth to tensile crack growth. The knee occurred in the range of 3–5 grain diameters.

(d) Kitagawa and Takahashi [27] and Taylor and Knott [28] used the stress range versus crack length curve to discriminate a microstructurally small crack from a mechanically small crack. For crack lengths > 500 µm, plots of the threshold stress range for fatigue crack growth ($\Delta\sigma_{th}$) versus crack length yield a straight line, i.e., the threshold stress intensity factor (ΔK_{th}) is constant. For crack lengths < 500 µm, $\Delta\sigma_{th}$ deviates from the linear relationship and approaches a constant value as the crack length becomes smaller. The constant value of $\Delta\sigma_{th}$ is approximately equal to the fatigue limit of a smooth specimen of the material. The crack length at which the $\Delta\sigma_{th}$ versus crack length curve changes from a linear relationship to a constant value is used to define the transition from microstructurally small to mechanically small cracks.

(e) Tokaji et al. [6,7,19] estimated the transition crack length to be ≈8 times the microstructural unit size. Ravichandran [29] reported that large fluctuations in crack shape or aspect ratio occur at crack lengths of about a few grain diameter (typically ≤5d, where d is grain diameter). Hussain et al. [17] observed that fatigue CGRs decreased systematically at microstructural heterogeneities up to a length of 3 to 4 grain diameters. Dowling [30] reported that the J-integral correlation is not valid for surface crack lengths < 10 crystallographic grain diameters.

The above studies indicate that the crack length for transition from MSC to mechanically small crack is a function of applied stress and microstucture of the material; actual value may range from 150 to 250 µm. A constant value of ≈200 µm was assumed for convenience, for both carbon and low–alloy steels; it is the initial size for mechanically small cracks.

FATIGUE CRACK GROWTH RATES

Air Environment

The growth rates da/dN (mm/cycle) of MSCs, i.e., from 10 to 200 µm, in air can be represented by the Hobson relationship [10,11,31,32]

$$da/dN = A_1\, (\Delta\sigma)^{n_1}\, (d - a), \quad (4)$$

where a is the length (mm) of the predominant crack, $\Delta\sigma$ is the stress range (MPa), constant A and exponent n are determined from existing fatigue S–N data, and d is the material constant related to grain size. The values of A_1 and n_1 for carbon and low–alloy steels at room temperature and reactor operating temperatures are given in Table 1. A value of 0.3 mm was used for the material constant d. Also, because growth rates increase significantly with decreasing crack lengths, a constant growth rate was assumed for crack lengths smaller than 0.075 mm. The applied stress range $\Delta\sigma$ is determined from Ramberg–Osgood relations given by Eqs. A1–A5 of the Appendix, it represents the value at fatigue half life.

Table 1. **Values of the constants A_I and n_I in Equation 4**

		A_I	n_I
Carbon Steels	Room Temp.	3.33×10^{-41}	13.13
	Operating Temp.	9.54×10^{-34}	10.03
Low–Alloy Steels	Room Temp.	1.45×10^{-36}	11.10
	Operating Temp.	1.07×10^{-43}	13.43

The growth rates of mechanically small cracks in air are estimated from Eq. A8 of the Appendix. A factor of 1.22 enhancement in growth rates was used at reactor operating temperatures.

LWR Environment

A model based on oxide film rupture and anodic dissolution (or slip dissolution/oxidation model) was proposed by Ford et al., [12] to incorporate the effects of LWR environments on fatigue lives of carbon and low–alloy steels. The model considers that a thermodynamically stable protective oxide film forms on the surface to ensure that the crack will propagate with a high aspect ratio without degrading into a blunt pit, and that a strain increment is required to rupture the oxide film, thereby exposing the underlying matrix to the environment. Once the passive oxide film is ruptured, crack extension is controlled by dissolution of freshly exposed surfaces and by the oxidation characteristics. Ford and Andresen [33] proposed that the average crack growth rate da/dt (cm/s) is related to the crack tip strain rate $\dot{\varepsilon}_{ct}$ (s^{-1}) by the relationship

$$da/dt = A_2 \left(\dot{\varepsilon}_{ct}\right)^{n_2}, \tag{5}$$

where constant A_2 and exponent n_2 depend on the material and environmental conditions at the crack tip. There is a lower limit of crack propagation rate associated with blunting when the crack tip cannot keep up with general corrosion rate of the crack sides or when a critical level of sulfide ions cannot be maintained at the crack tip. The crack propagation rate at which this transition occurs may depend on dissolved oxygen level, flow rate, etc. Based on these factors, the maximum and minimum environmentally assisted crack propagation rates have been defined [12,33,34]. For crack–tip sulfide ion concentrations above the critical level, CGR is expressed as

$$da/dt = 2.25 \times 10^{-4}(\dot{\varepsilon}_{ct})^{0.35} \tag{6a}$$

and for crack–tip sulfide ion concentrations below the critical level, CGR is expressed as

$$da/dt = 10^{-2}(\dot{\varepsilon}_{ct})^{1.0}. \tag{6b}$$

However, the growth rates predicted by Eqs. 6a and 6b are somewhat higher than those observed experimentally [8]. To be consistent with the experimental data, the constants in Eqs. 6a and 6b were decreased by a factor of 3.2 and 2.5, respectively. Assuming that the crack–tip strain rate, $\dot{\varepsilon}_{ct}$, is approximately the same as the applied strain rate, $\dot{\varepsilon}_{app}$, and crack advance due to mechanical fatigue is insignificant during the initial stages of fatigue damage, crack advance per cycle from Eq. 6a for significant environmental effects is given by

$$da/dN = 7.03 \times 10^{-5}(\Delta\varepsilon - \varepsilon_f)(\dot{\varepsilon}_{app})^{-0.65}, \tag{7a}$$

and from Eq. 6b for moderate environmental effects is given by

$$da/dN = 4.00 \times 10^{-3}(\Delta\varepsilon - \varepsilon_f), \tag{7b}$$

where $\dot{\varepsilon}_{app}$ is the applied strain rate (s^{-1}) and ε_f is the threshold strain range needed to rupture the oxide film; ε_f was assumed to be 0.0023 and 0.0029, respectively, for carbon steels and low–alloy steels. For strain rates greater than ≈0.3%/s, da/dN from Eq. 7a is lower than that from Eq. 7b. Also, existing fatigue S–N data indicate that strain rate effects on life saturate at ≈0.001%/s [2]. Therefore, Eq. 7a is applicable for applied strain rates between 0.003 and 0.00001 s^{-1}, $\dot{\varepsilon}_{app}$ is assumed to be 0.003 s^{-1} for higher values, and 0.00001 s^{-1} for lower values. Equations 7a and 7b consider that the stress–free state for the surface oxide film is at peak compressive stress.

Studies on crack initiation and crack growth in smooth fatigue specimens indicate that the reference fatigue CGR curves (Fig. A1) for carbon and low–alloy steels in LWR environments are somewhat higher than those determined experimentally from the growth of mechanically small cracks in LWR environments [8]. Furthermore, using the reference CGR curves and fracture mechanics analyses to examine the fatigue S-N behavior of these steels in LWR environments yields conservative results. Therefore, the reference fatigue CGR curves were modified to estimate the growth rates of mechanically small cracks; the modified curves are shown in Fig. 2. The threshold values of ΔK (MPa·m$^{1/2}$) are given by

$$\Delta K_b = 10.11\ \theta^{0.326}, \tag{8a}$$

$$\Delta K_c = 32.03\ \theta^{0.326}, \tag{8b}$$

where rise time θ is in seconds.

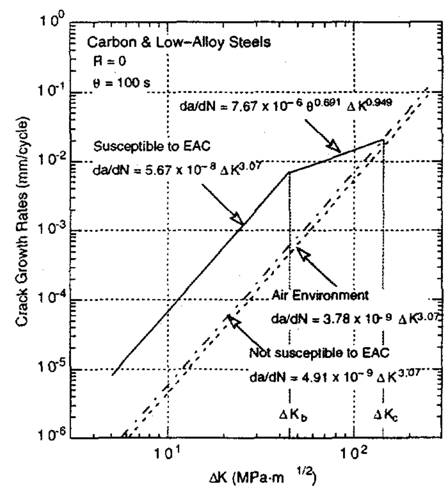

Figure 2. Modified reference fatigue crack growth rate curves for carbon and low–alloy steels for LWR applications

Environmental effects on fatigue life are moderate when any one of the threshold environmental conditions is not satisfied, e.g., temperature <150°C, DO <0.05 ppm, strain rate >1%/s, or strain range is below the critical value. For moderate environmental effects, the growth rates of mechanically small cracks are represented by the curves for materials not susceptible to environmentally assisted cracking (EAC), and those of MSCs by either Eq. 7b or Eq. 4, whichever yields the higher value. For example, at high strain ranges, growth rates determined from Eq. 4 can be higher than those determined from Eq. 7b, i.e., mechanical factors control crack growth and environmental effects are insignificant.

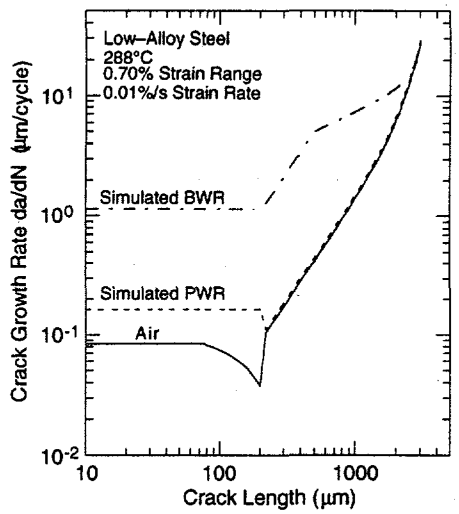

Figure 3. Crack growth rates during fatigue crack initiation in low–alloy steels in air and simulated PWR and BWR environments

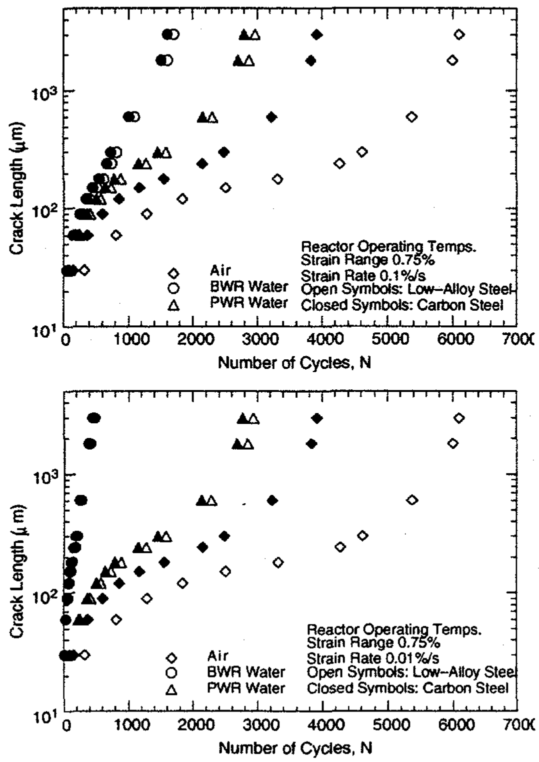

Figure 4. Crack growth as a function of fatigue cycles

Environmental effects on fatigue life are significant when all of the threshold conditions are satisfied, e.g., temperature ≥150°C, DO ≥0.05 ppm, strain rate <1%/s, and strain range is above the critical value. A minimum threshold S content of 0.005 wt.% was also considered, i.e., S content must also be >0.005 wt.% for significant environmental effects on fatigue life. When all five threshold conditions are satisfied, the growth rates of mechanically small cracks are represented by the curve for materials susceptible to EAC for ΔK values below ΔK_b, by the curve for materials not susceptible to EAC at ΔK values above ΔK_c, and by the transition curve for in–between values of ΔK. The growth rates of MSCs are represented by either Eq. 7a or Eq. 4, whichever yields the higher value.

ESTIMATES OF FATIGUE LIFE

The existing fatigue S–N data for carbon and low–alloy steels in air and LWR environments were examined with the present model, which considers fatigue life to consist of the growth of (a) MSCs and (b) mechanically small cracks. The former may be defined as the "initiation" stage and represents the growth of MSCs from 10–200 µm. The growth of mechanically small cracks may be defined as the "propagation" stage and represents the growth of fatigue cracks from 200–3000 µm. During initiation stage, the growth of MSCs is expressed by a modified Hobson relationship in air (Eq. 4) and by the slip dissolution/oxidation process in water (Eqs. 7a or 7b). During propagation stage, the growth of mechanically small cracks is characterized in terms of the J–integral range ΔJ and CGR data in air and LWR environments (Fig. 2). The correlations for calculating the stress range, stress intensity range ΔK, J–integral range ΔJ, and the CGRs for long cracks in air are given in the appendix. For the cylindrical fatigue specimens, the stress intensity ranges ΔK were determined from the values of J–integral range ΔJ. Although, ΔJ is often computed only for that portion of the loading cycle during which the crack is open, in the present study, the entire hysteresis loop was used in estimating ΔJ [30]. The stress intensities associated with conventional cylindrical fatigue specimens were modified according to the correlations developed by O'Donnell and O'Donnell [35]. Typical CGRs and crack growth behavior during fatigue crack initiation in air and water environments are shown in Figs. 3 and 4, respectively.

Experimental values of fatigue life and those predicted from the present model in air and low– and high–DO water are plotted in Fig. 5. The fatigue S–N curves developed from the present model and those obtained from Eqs. 1–3 in air and water environments are shown in Figs. 6 and 7, respectively. The predicted fatigue lives in air show excellent agreement with the experimental data; the predicted values in LWR environments, particularly in high–DO water, are slightly lower than the experimental values. The results seem to imply that, in water, the data obtained from smooth fatigue specimens may not be conservative in the high-cycle regime, i.e., at low strain amplitudes.

CONCLUSIONS

A fracture mechanics approach has been used to predict the fatigue lives of carbon and low-alloy steels in air and LWR environments. The present model considers fatigue life to be composed of the growth of (a) microstructurally small cracks that is very sensitive to microstructure and is characterized by decelerating crack growth, and (b) mechanically small cracks that can be predicted by fracture mechanics methodology and is characterized by accelerating crack growth. The growth of the latter has been characterized in terms of the J–integral range ΔJ and CGR data in air and LWR environments. The growth of microstructurally small cracks is expressed by a modified Hobson relationship in air and by the slip dissolution/oxidation process in water. The crack length for transition

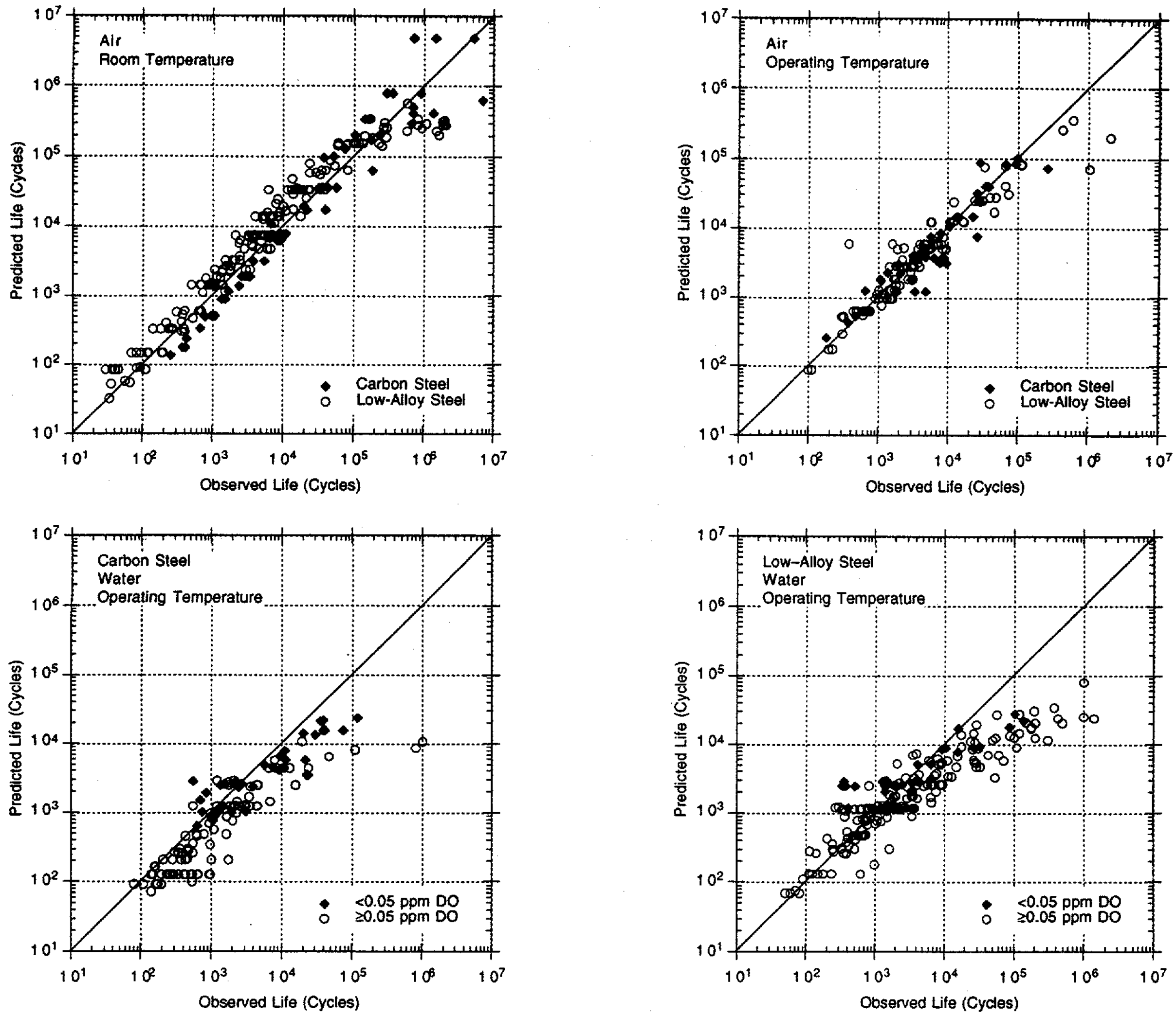

Figure 5. Experimentally observed values of fatigue life vs. those predicted by the present model in air and water environments

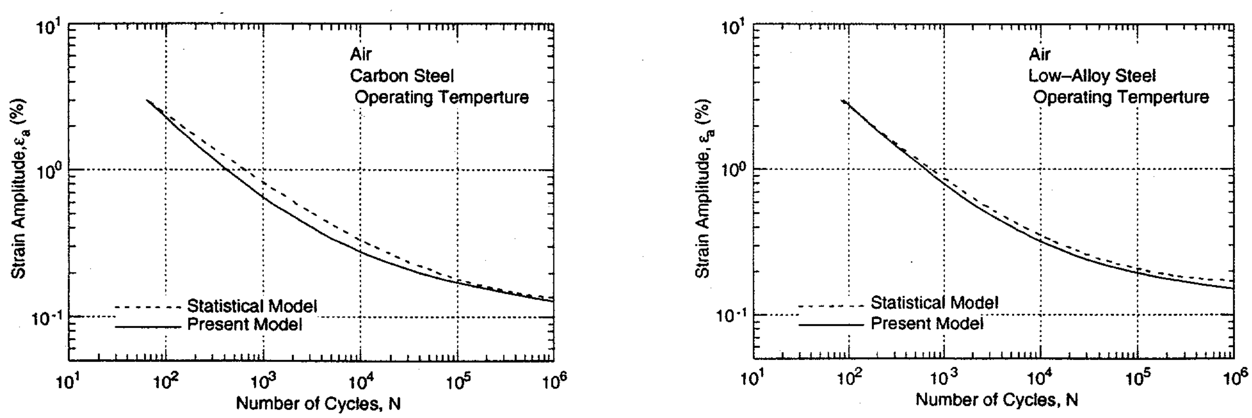

Figure 6. Fatigue strain vs. life curves developed from the present model for carbon and low-alloy steels in air

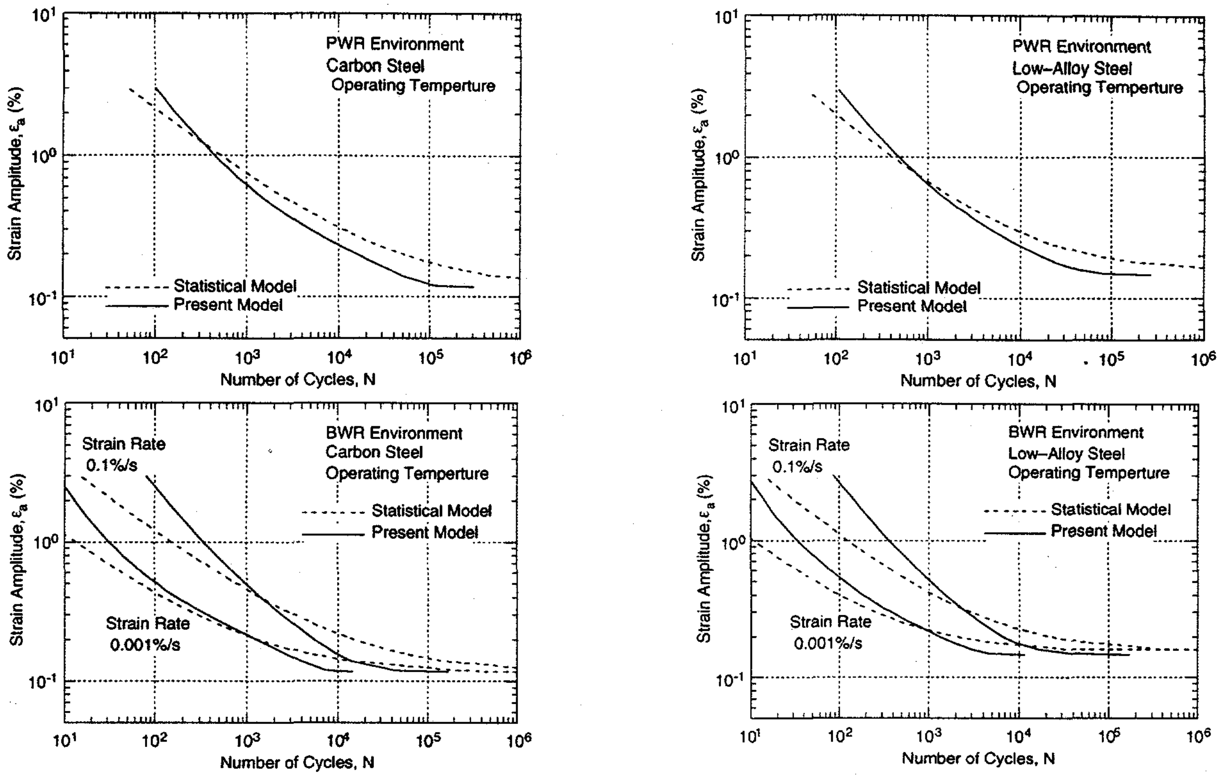

Figure 7. Fatigue strain vs. life curves developed from the present model for carbon and low–alloy steels in LWR environments

from microstructurally small crack to mechanically small crack was based on studies on small crack growth.. Fatigue lives estimated from the present model show good agreement with the experimental data for carbon and low–alloy steels in air and LWR environments. At low strain amplitudes, i.e., fatigue lives $>10^4$ cycles, the predicted lives in water can be significantly lower than those observed experimentally.

ACKNOWLEDGMENTS

This work was supported by the International Atomic Energy Agency Fellowship Program, administered by the National Academy of Sciences – National Research Council, under a contract with the U.S. Government.

APPENDIX

Cyclic Stress Range

The cyclic stress–strain response of carbon and low–alloy steels varies with steel type, temperature, and strain rate. In general, these steels exhibit initial cyclic hardening, followed by cyclic softening or a saturation stage. The carbon steels, with a pearlite and ferrite structure and low yield stress, show significant initial hardening. The low–alloy steels, which consist of tempered ferrite and a bainite structure, have a relatively high yield stress, and show little or no initial hardening, may exhibit cyclic softening at high strain ranges. At 200–370°C, these steels exhibit dynamic strain aging, which results in enhanced cyclic hardening, a secondary hardening stage, and negative strain rate sensitivity. Under the conditions of dynamic strain aging, cyclic stress increases with decreases in strain rate.

The cyclic stress range vs. strain range relationship is expressed by the modified Ramberg–Osgood relationship given by

$$\Delta\varepsilon = \left(\Delta\sigma/E\right) + \left(\Delta\sigma/A_3\right)^{n_3}, \qquad \text{(A1)}$$

where E is Young's modulus, constant A_3 and exponent n_3 are determined from the experimental data, and cyclic stress range corresponds to the value at half–life. At room temperature, the cyclic stress range $\Delta\sigma$ (MPa) and strain range $\Delta\varepsilon$ (%) relationship for carbon steel may be represented by

$$\Delta\varepsilon = (\Delta\sigma/2010) + (\Delta\sigma/766.1)^{(1/0.207)}, \qquad \text{(A2)}$$

and for low–alloy steels by

$$\Delta\varepsilon = (\Delta\sigma/2010) + (\Delta\sigma/847.4)^{(1/0.173)}. \qquad \text{(A3)}$$

The effect of strain rate on the cyclic stress–strain curve is not considered at room temperature. At 288°C, the cyclic stress–strain curves may be represented by the correlations developed by Chopra and Shack [2]. For carbon steels, the curve is given by the relation

$$\Delta\varepsilon = (\Delta\sigma/1965) + (\Delta\sigma/\mathrm{Asig})^{(1/0.129)}, \qquad \text{(A4a)}$$

where Asig varies with the strain rate $\dot{\varepsilon}$ (%/s) expressed as

$$\mathrm{Asig} = 1079.7 - 50.9\log(\dot{\varepsilon}). \qquad \text{(A4b)}$$

For low–alloy steels, the curve is given by the relation

$$\Delta\varepsilon = (\Delta\sigma/1965) + (\Delta\sigma/\mathrm{Bsig})^{(1/0.110)}, \qquad \text{(A5a)}$$

where Bsig is expressed as

$$\mathrm{Bsig} = 961.8 - 30.3\log(\dot{\varepsilon}). \qquad \text{(A5b)}$$

Stress Intensity Factor Range

For cylindrical fatigue specimens, the range of stress intensity factor ΔK, was determined from the value of J–integral range ΔJ, which for a small semi-circular surface crack is given by [30]

$$\Delta J = 3.2\,(\Delta\sigma^2/2E)\,a + 5\,[\Delta\sigma\,\Delta\varepsilon_p/(S + 1)]\,a \tag{A6a}$$

where $\Delta\varepsilon_p$ is plastic strain range (%) (second term in the Ramberg Osgood relationship) and S is the reciprocal of the strain hardening exponent n in Eq. A1. The stress intensity factor range ΔK is obtained from

$$\Delta K = (E\,\Delta J)^{1/2} \tag{A6b}$$

where E is the elastic modulus. Equation A6a incorporates a combined surface and flaw shape correction factor F_S of 0.714, which is derived from equivalent linear elastic solutions; Eq. 6a is valid as long as the crack size is very small compared to the specimen diameter. For conventional fatigue tests, life is defined as the number of cycles for the tensile stress to decrease 25% from the peak or steady–state value, i.e., the crack depth–to–specimen diameter ratio can be as high as 0.4. Therefore, the geometrical correction factor F_s for a small semi–circular surface crack was modified according to the correlation developed by O'Donnell and O'Donnell [35]:

$$F_s = 0.6911 + 1.2685\,(a/D) - 5.6638\,(a/D)^2 + 21.511\,(a/D)^3, \tag{A7}$$

where D is specimen diameter. For conventional fatigue tests on cylindrical specimens, F_s may increase up to 1.7 [35].

The J–integral range ΔJ is calculated from the ranges of stress and plastic strain, determined from stable hysteresis loops, i.e., at fatigue half life. In general, ΔJ is computed only for that portion of the loading cycle during which the crack is open. For fully reversed cyclic loading, the crack opening point can be identified as the point where the curvature of the load–vs.–displacement line changed prior to the peak compressive load. In the present study, evidence of crack opening point was observed for cracks that had grown relatively large, i.e., near the end of fatigue life. Therefore, as recommended by Dowling [30], the entire hysteresis loop was used in estimating ΔJ.

Crack Growth Rate

The fatigue CGRs da/dN of structural materials are characterized in terms of the range of applied stress intensity factor ΔK and are given in Article A–4300 of Section XI of the ASME Boiler and Pressure Vessel Code. For stress ratio R in the range of $-2 < R < 0$, the reference fatigue CGRs da/dN (mm/cycle) of carbon and low–alloys steels exposed to air environments are given by

$$da/dN = 3.78 \times 10^{-9}\,(\Delta K)^{3.07}, \tag{A8}$$

where $\Delta K = K_{max}$ the max stress intensity factor ($MPa{\cdot}m^{1/2}$). However, the effect of temperature is not considered in Eq. A8; CGRs are generally higher at 288°C than at room temperature [36]. The results of Logsdon and Liaw [36] indicate that for both carbon and low–alloy steels, CGRs at 288°C are ≈22% higher than those at room temperature.

Section XI of the ASME Code also includes CGR curves for these steels exposed to LWR environments. The growth rates are represented by two curves for low and high values of ΔK. However, the curves do not consider the effects of loading rate. Recent experimental results have shown the importance of key variables of material, environment, and loading rate on CGRs in LWR environments. Fatigue CGR correlations have been developed to explicitly consider the effects of loading rate, stress ratio R, ΔK, and S content in the steel [37]. The new correlations, shown in Fig. A1, are divided into two categories: (a) for materials not susceptible to environmental effects, e.g., low S content in the steel, CGRs are a factor of 2.8 higher than those in air; and (b) for materials susceptible to environmental effects, e.g., high S content in the steel, CGRs are defined in terms of rise time θ, stress ratio R, and ΔK.

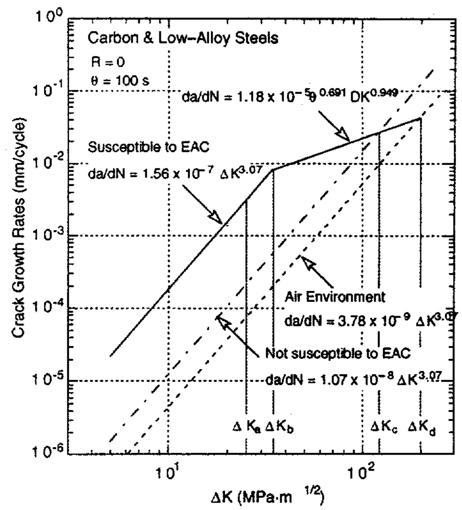

Figure A1. Proposed reference fatigue crack growth rate curves for carbon and low–alloy steels in LWR environments for a rise time of 100 s and R = –1

The correlations in Fig. A1 correspond to a rise time of 100 s and $K_{min} < 0$, e.g., fully reversed cyclic loading; R is set to zero. The various threshold values of ΔK ($MPa{\cdot}m^{1/2}$) are given by

$$\Delta K_a = 14.156\,\theta^{0.125}, \tag{A9a}$$

$$\Delta K_b = 7.691\,\theta^{0.326}, \tag{A9b}$$

$$\Delta K_c = 27.186\,\theta^{0.326}, \tag{A9c}$$

$$\Delta K_d = 44.308\,\theta^{0.326}, \tag{A9d}$$

where rise time θ is in seconds.

REFERENCES

1. Chopra, O. K., and Shack, W. J., 1997, "Evaluation of Effects of LWR Coolant Environments on Fatigue Life of Carbon and Low–Alloy Steels," *Effects of the Environment on the Initiation of Crack Growth*, ASTM **STP 1298**, W. A. Van Der Sluys, R. S. Piascik, and R. Zawierucha, eds., American Society for Testing and Materials, Philadelphia, pp. 247–266.
2. Chopra, O. K., and Shack, W. J., 1998a, *Effects of LWR Coolant Environments on Fatigue Design Curves of Carbon and Low-Alloy Steels*, NUREC/CR-6583, ANL-97/18.

3. Chopra, O. K., and Shack, W. J., 1998b, "Low-Cycle Fatigue of Piping and Pressure Vessel Steels in LWR Environments," *Nucl. Eng. Des.* **184**, pp. 49-76.
4. Chopra, O. K., and Shack, W. J., 1998c, "Fatigue Crack Initiation in Carbon and Low-Alloy Steels in Light Water Reactor Environments – Mechanism and Prediction," *Fatigue, Environmental Factors, and New Materials*, PVP **374**, ASME, pp. 155-168.
5. Chopra, O. K., and Shack, W. J., 1999, "Overview of Fatigue Crack Initiation in Carbon and Low-Alloy Steels in LWR Environments," *J. Pressure Vessel Technology* **121**, pp. 49-60.
6. Tokaji, K., Ogawa, T., and Harada, Y., 1986b, "The Growth of Small Fatigue Cracks in a Low Carbon Steel; The Effect of Microstructure and Limitation of Linear Elastic Fracture Mechanics," *Fatigue Fract. Engng. Mater. Struct.* **9**, pp. 205-217.
7. Tokaji, K., Ogawa, T., and Osako, S., 1988, "The Growth of Microstructurally Small Fatigue Cracks in a Ferrite-Bainitic Steel," *Fatigue Fract. Engng. Mater. Struct.* **11**, pp. 331-342.
8. Gavenda, D. J., Luebbers, P. R., and Chopra, O. K., 1997, "Crack Initiation and Growth Behavior of Carbon and Low-Alloy Steels," *Fatigue and Fracture 1*, PVP **350**, ASME, pp. 243-255.
9. Suh, C. M., Yuuki, R., and Kitagawa, H., 1985, "Fatigue Microcracks in a Low Carbon Steel," *Fatigue Fract. Engng. Mater. Struct.* **8**, pp. 193-203.
10. Hobson, P. D., 1982, "The Formulation of a Crack Growth Equation for Short Cracks," *Fatigue Fract. Engng. Mater. Struct.* **5**, pp. 323-327.
11. Miller, K. J., 1985, "Initiation and Growth Rates of Short Fatigue Cracks," *Fundamentals of Deformation and Fracture*, Cambridge Press, pp. 477-500.
12. Ford, F. P., Ranganath, S., and Weinstein, D., 1993, *Environmentally Assisted Fatigue Crack Initiation in Low–Alloy Steels – A Review of the Literature and the ASME Code Requirements*, EPRI Report TR–102765.
13. Higuchi, M., and Iida, K., 1991, "Fatigue Strength Correction Factors for Carbon and Low–Alloy Steels in Oxygen–Containing High–Temperature Water," *Nucl. Eng. Des.* **129**, pp. 293–306.
14. Higuchi, M., Iida, K., and Asada, Y., 1997, "Effects of Strain Rate Change on Fatigue Life of Carbon Steel in High–Temperature Water," *Effects of the Environment on the Initiation of Crack Growth*, ASTM **STP 1298**, W. A. Van Der Sluys, R. S. Piascik, and R. Zawierucha, eds., American Society for Testing and Materials, Philadelphia, pp. 216–231.
15. Higuchi, M., 1995, presented at Working Group Meeting on S–N Data Analysis, the Pressure Vessel Research Council, June, Milwaukee.
16. Smith, R. A., Liu, Y., and Garbowski, L., 1996, "Short Fatigue Crack Growth Behavior in Waspaloy at Room and Elevated Temperature," *Fatigue Fract. Engng. Mater. Struct.* **19**, pp. 1505-1514.
17. Hussain, K., Tauqir, A., Hashmi, S. M., and Khan, A. Q., 1994, "Short Fatigue Crack Growth Behavior in Ferrite-Bainitic Steel," *Metall. Trans. A* **25A**, pp. 2421-2425.
18. Tokaji, K., Ogawa, T., Harada, Y., and Ando, Z., 1986a, "Limitation of Linear Elastic Fracture Mechanics in Respect of Small Fatigue Cracks and Microstructure," *Fatigue Fract. Engng. Mater. Struct.* **9**, pp. 1-14.
19. Tokaji, K., and Ogawa, T., 1992, "The Growth Behavior of Microstructurally Small Fatigue Cracks in Metals," *Short Fatigue Cracks*, ESIS 13, Mechanical Engineering Pub., pp. 85-99.
20. Suh, C. M., Lee, J. J., and Kang, Y. G., 1990, "Fatigue Microcracks in Type 304 Stainless Steel at Elevated Temperature," *Fatigue Fract. Engng. Mater. Struct.* **13**, pp. 487-496.
21. de los Rios, E. R., Navarro, A., and Hussain, K., 1992, "Microstructural Variations in Short Fatigue Crack Propagation of a C-Mn Steel," *Short Fatigue Cracks*, ESIS 13, Mechanical Engineering Pub., pp. 115-132.
22. de los Rios., Wu, X. D., and Miller, K. J., 1996, "A Micro-Mechanics Model of Corrosion-Fatigue Crack Growth in Steels," *Fatigue Fract. Engng. Mater. Struct.* **19**, pp. 1383-1400.
23. Lankford, J., 1977, "Initiation and Early Growth of Fatigue Cracks in High Strength Steels," *Eng. Fract. Mech.* **9**, pp. 617-624.
24. Lankford, J., 1982, "The Growth of Small Fatigue Cracks in 7075-T6 Aluminum," *Fatigue Fract. Engng. Mater. Struct.* **5**, pp. 233-248.
25. Lankford, J., 1985, "The Influence of Microstructure on The Growth of Small Fatigue Cracks," *Fatigue Fract. Engng. Mater. Struct.* **8**, pp. 161-175.
26. Obrtlik, K., Polak, J., Hajek, M., and Vasek, A., 1997, "Short Fatigue Crack Behavior in 316L Stainless Steel," *Int. J. Fatigue* **19**, pp. 471-475.
27. Kitagawa, H., and Takahashi, S., 1976, "Applicability of Fracture Mechanics to Very Small Cracks of the Cracks in the Early Stage," *Proc. 2nd Int. Conf. on Mechanical Behavior of Materials*, ASM, pp. 627-631.
28. Taylor, D., and Knott, J. F., 1981, "Fatigue Crack Propagation Behavior of Short Cracks; The Effect of Microstructure," *Fatigue Fract. Engng. Mater. Struct.* **4**, pp. 147-155.
29. Ravichandran, K. S., 1997, "Effects of Crack Aspect Ratio on the Behavior of Small Surface Cracks in Fatigue; Part II. Experiments on a Titanium (Ti-8Al) Alloy," *Metall. Trans. A* **28A**, pp. 157-167.
30. Dowling, N. E, 1977, "Crack Growth During Low-Cycle Fatigue of Smooth Axial Specimens," ASTM **STP 637**, pp. 97-121.
31. Carbonell, E. P., and Brown, M. W., 1986, "A Study of Short Crack Growth in Torsional Low Cycle Fatigue for a Medium Carbon Steel," *Fatigue Fract. Engng. Mater. Struct.* **9**, pp. 15-33.
32. Brown, M. W., 1986, "Interface Between Short, Long and Non-Propagating Cracks," *Mechanical Engineering Pub.*, pp. 423-439.
33. Ford, F. P., and Andresen, P. L, 1995, *Corrosion in Nuclear Systems: Environmentally Assisted Cracking in Light Water Reactors*, Marcel Dekker Inc., pp. 501-546.
34. Ford, F. P., 1996, "Quantitative Prediction of Environmentally Assisted Cracking," *Corrosion* **52**, pp. 375-395.
35. O'Donnell, T. P., and O'Donnell, W. J., 1995, "Stress Intensity Values in Conventional S-N Fatigue Specimens," *Intnl. Pressure Vessels and Piping Codes and Standards*, PVP **313**, pp. 195-197.
36. Logsdon, W. A., and Liaw, P. K., 1985, "Fatigue Crack Growth Rate Properties of SA508 and SA533 Pressure Vessel Steels and Submerged Arc Weldments in Room and Elevated Temperature Air Environments," *Eng. Frac. Mech.* **22**, pp. 509-526.
37. Eason, E. D., Nelson E. E., and Gilman, J. D., 1994, "Modeling of Fatigue Crack Growth Rate for Ferritic Steels in Light Water Reactor Environments," *Changing Priorities of Code and Standards*, PVP **286**, ASME, pp. 131–142.